Exploring Spatial Patterns of Emergency Call Behavior in a Metropolitan City of China

Ning Yuan[1(✉)], Bo Yang[2], Kun Fu[2], Lei Du[1], Pengfei Jiao[3], Lin Pan[4], Qiang Tian[5], and Wenjun Wang[6]

[1] Tianjin Zhongtian Huitong Technology Co., Ltd., Tianjin 300121, China
yuanning@witapex.cn
[2] China Mobile Communications Group Jiangxi Co., Ltd., Nanchang 330038, China
[3] School of Cyberspace, Hangzhou Dianzi University, Hangzhou 310018, China
[4] School of Marine Science and Technology, Tianjin University, Tianjin 300072, China
[5] Computer and Information Engineering College, Tianjin Normal University, Tianjin 300382, China
[6] College of Intelligence and Computing, Tianjin University, Tianjin 300350, China

Abstract. Extensive analysis of human electronic footprints is of great importance for unveiling the patterns of collective reactions to extreme events. Several empirical results have been reported to reveal the influence of different scale events on human behavior using various social media datasets. But there is a lack of understanding of the patterns of emergency call behavior which is the direct evidence of unexpected events encountered by citizens. Here we explore the spatial patterns of emergency calls made by citizens in a metropolitan city in China. We find that there is strong randomness in the spatial conversion of emergency call behavior, the number of emergency calls made by an individual in a specific location of an incident follows a power-law distribution, and the spatial pattern of incident locations presents a bi-central aggregation feature. Then we propose an agent based model for the generation of incident location series. Our work has the potential value to help the government improve the efficiency of emergency management such as situation analysis, resource allocation and police deployment.

Keywords: Spatial pattern · Emergency call · Random walk model · Human behavior simulation

1 Introduction

With the wide application of mobile phones and other social media, human behavior can be aware through these electronic footprint data sets, which provide

Supported by the National Natural Science Foundation of China (61902278 and 62102262) and the National Key R&D Program of Jiangxi, China (20212ABC03W12).

Y. Chenggang et al. (Eds.): MobiMedia 2022, LNICST 451, pp. 269–283, 2022.
https://doi.org/10.1007/978-3-031-23902-1_21

multi-dimensional information for quantitative research on human dynamics [3, 6,8,30]. Moreover, on the basis of the study of normal human behavior, many researchers have carried out exploratory studies on the influence of unexpected events on spatiotemporal patterns of human behavior in recent years. Their work is of great importance to improving the efficiency of emergency management for governments [16].

Some anomalies that are triggered by different scale of emergencies, including sharp increased call volume [2,11,20], shortened call duration [20], anomalous information diffusion [11], unusual travel pattern [19–21], higher mobility predictability [19] and social activity [2,20], have been uncovered using mobile phone records and applied in anomaly detection [1,5,7,26]. Some other datasets such as Flicker [22], Twitter [18,25,27], Facebook [25], GPS [23,24] and Air Transportation Network [29] are also used to study the influence of disasters on social communication or human mobility [10]. Meanwhile, emergency call records (ECR), which is considered as the direct evidence dataset of unexpected events encountered by citizens, has been studied for sociological perspective verification [9], hot spots analysis [14], event detection [13,15] and call center workload prediction [4]. However, there is a lack of extensive understanding of the spatiotemporal patterns of emergency call behavior [12,14,28].

In this paper, we studied the spatial patterns of emergency calls made by citizens in a city in China. The character of strong randomness was found in the spatial conversion of emergency call behavior. The number of emergency calls made by an individual in a specific location of incident was detected to follow a power-law distribution, and the spatial pattern of incident locations presented a feature of bi-central aggregation. Then we proposed an agent based model for the generation of incident location series. Our work has potential value in applications in emergency management.

2 Materials and Methods

2.1 Dataset Description

To study the temporal dynamic of calling behavior in case of emergency, we applied for the right to use two datasets which have been encrypted to eliminate personal privacy:

(a) A dataset of ECR collected from a metropolitan city in China from Jan. 1, 2008 to Dec. 3, 2012. It contains a total of 22,358,046 incoming calls from 7,724,005 distinct phone numbers.
(b) A mobile phone signaling dataset from a Chinese operator covering ∼2 billion calling records of ∼6 million users in the city, same as dataset (a) from August 1, 2011 to October 31, 2011.

2.2 Methods

Data Preprocessing. We have collected the geographic coordinates of the incident locations from valid emergency call records in dataset (a). We focused our study on urban areas and finally obtained a dataset of 4,836,065 emergency call records with valid incident locations from 2,357,361 individuals.

The home and workplace of the individuals were extracted from dataset (b) using the similar method as described in [17]. Differently, we assigned the daytime and nighttime periods with 9 a.m. to 5 p.m. and 10 p.m. to 6 a.m. on weekdays, respectively to identify home and workplace.

Statistics for Incident Locations. The displacement Δr is defined as the distance between two consecutive incident locations of an individual. The trajectory of emergency call behavior is formed by an individual's consecutive incident locations, and its radius of gyration is defined as

$$r_g = \sqrt{\frac{1}{C}\sum_{i=1}^{C}(\overrightarrow{r_i} - \overrightarrow{r_{cm}})^2}, \tag{1}$$

where $\overrightarrow{r_i}$ represents the $i = 1, \ldots, C$ incident locations recorded for the individual and $\overrightarrow{r_{cm}} = \frac{1}{C}\sum_{i=1}^{C}\overrightarrow{r_i}$ is the center of mass of the trajectory.

The number of incident locations in one trajectory is denoted as L to measure the spatial activity of emergency calls for an individual. The number of emergency calls made at a single incident location is denoted as C_L to measure the emergency call activity at a fixed position for the individual.

Location Normalization. For investigating the aggregation characteristics of emergency call behavior, we took home and workplace as two reference points. A new coordinate system was constructed by mapping the geographic coordinates of each individual's home and workplace to $(-1, 0)$ and $(1, 0)$, respectively. Then an incident location could be mapped to a point in the new coordinate system according to its relative position to one's home and workplace points. Moreover, each incident location was classified as its nearer reference center defined as the origin point of a single step. And the displacement from home(workplace) to an incident location was denoted as D_h (D_w). The angle between the direction of home (workplace) to an incident location and the commuting direction counterclockwise is denoted as θ_h (θ_w). The number of home (workplace) that consecutive occurrenced in the series of reference centers for an individual is denoted as n_h (n_w).

Fit Test for Simulation Analysis. The original definition of Kullback-Leibler divergence is a non-symmetric measure of the difference between two probability distributions P and Q:

$$KL(P \parallel Q) = \sum_i P(i) \log \frac{P(i)}{Q(i)}. \tag{2}$$

To evaluate the goodness-of-fit for statistical characteristics of simulation data, the symmetrical divergence was adopted here as:

$$D(P \parallel Q) = \frac{1}{2}(KL(P \parallel Q) + KL(Q \parallel P)). \tag{3}$$

Further, we specified the discrete random variable $x^{(m)}, m = 1, 2, \ldots, M$, whose distribution in real data is $P(x^{(m)})$, and $Q(x^{(m)}|\varphi^{(n)})$ is the distribution of simulation data generated under N groups of parameters $\varphi^{(n)}, n = 1, 2, \ldots, N$. Then the relative fitting deviation for distribution $P(x^{(m)})$ to $Q(x^{(m)})$ under the parameter set $\varphi^{(n)}$ is defined as:

$$R(X^{(m)}|\varphi^{(n)}) = \frac{D(P(X^{(m)}) \parallel Q(X^{(m)}|\varphi^{(n)}))}{\frac{1}{N}\sum_{n=1}^{N} D(P(X^{(m)}) \parallel Q(X^{(m)}|\varphi^{(n)}))}. \tag{4}$$

For the probability distribution of all random variables $x^{(m)}$ used for evaluation, the average relative fitting deviation of the model under the parameter set $\varphi^{(n)}$ is:

$$\langle R \rangle(\varphi^{(n)}) = \frac{1}{M}\sum_{m=1}^{M} R(X^{(m)}|\varphi^{(n)}), \tag{5}$$

which will be used as the basis for parameter optimization.

3 Empirical Results

3.1 Spatial Patterns of Emergency Call Behavior

To explore the spatial patterns of emergency call behavior, we studied the ECR data set in the urban area of a metropolitan city in China for five years. The distributions of displacement (Δr) and radius of gyration (r_g) of trajectories formed by incident locations were very consistent for different years. We tested the fitnesses of these two distributions with functions of power-law (POW), exponent (EXP), truncated power-law (TPL) and gauss (GAU), respectively. It was shown that the distributions $P(\Delta r)$ and $P(r_g)$ could be well fitted by the gauss function $P(x) = \frac{A}{\sqrt{2\pi}\sigma}\exp\left(-\frac{(x+\mu)^2)}{2\sigma^2}\right)$, where $A = 4.021, \mu = 8.873, \sigma = 8.989$ for $P(\Delta r)$ and $A = 0.385, \mu = 0.003, \sigma = 3.279$ for $P(r_g)$, respectively (See Fig. 1). It indicated that there was a strong randomness in the spatial pattern of emergency call behavior.

The number of incident locations for an individual (L) was considered to evaluate the activity of encountering emergency events. The distributions of L at the aggregated level for different years were observed as a consistent power-law decay $P(L) \sim L^{-\alpha}$, where $\alpha \approx 3.75$ as shown in Fig. 2 (a). Meanwhile, the number of emergency calls in a single incident location for an individual (C_L) also followed a power-law distribution $P(C_L) \sim C_L^{-\beta}$, where $\beta \approx 3.29$ as shown in

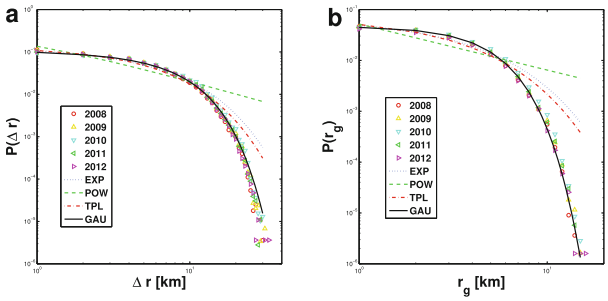

Fig. 1. Distributions of Δr and r_g in the log-log scale at aggregated level for different years. The tested fitting functions of exponent (EXP), power-law (POW), truncated power-law (TPL) and gauss (GAU) are shown as blue dot, green dashed, red dot-dashed and black solid curves, respectively. (Color figure online)

Fig. 2 (b). These phenomena indicate that the activity of emergency call behavior is very inhomogeneous for individuals. Then we studied the trends of average values of displacement (Δr), radius of gyration (r_g) and the number of emergency calls (C_i) for groups of individuals with the increase of L by 1 km interval. As shown in Fig. 2 (c), $\langle \Delta r \rangle$ and $\langle r_g \rangle$ increased rapidly and then tended to be saturated at about 4 km. It indicated that the number of events that an individual encountered averagely almost had no effect on the basic spatial patterns of emergency call behavior. And the saturation value should be associated to the scope of studied urban areas. As shown in Fig. 2 (d), $\langle C_i \rangle$ presented positive linear correlation with L as $\langle C_i \rangle = kL$, where $k = 1.25$.

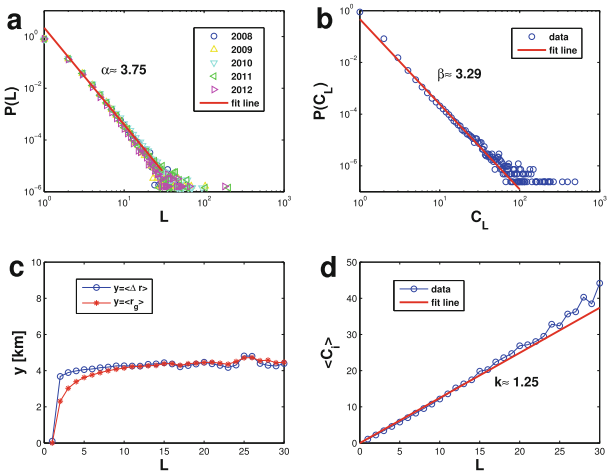

Fig. 2. (a) and (b) are the distribution of L and C_L in the log-log scale at the aggregated level. (c) and (d) shows the trends of $\langle \Delta r \rangle$, $\langle \Delta r \rangle$ and $\langle C_i \rangle$ for groups with different L.

3.2 Relative Position of Incident Location

Furthermore, we investigated the potential nonrandom characteristics in emergency call behavior. Considering the randomness of emergency events that individuals encountered, the generation of incident locations was not a strict continuous process, but occured randomly around the specific centers of their daily travel. In order to verify this hypothesis, we studied the characteristics of relative positions of incident locations, taking home and workplace for reference. Incident locations were transformed to a new coordinate system as described in Subsect. 2.2. The incident location points were separated into four groups by individuals with commuting distance (D_c) in different ranges of $0\,\text{km} \leq D_c \leq 5\,\text{km}$, $5\,\text{km} < D_c \leq 10\,\text{km}$, $10\,\text{km} < D_c \leq 20\,\text{km}$, $20\,\text{km} < D_c \leq 30\,\text{km}$, respectively. The normalized value of the number of incident location points in each grid of 0.1×0.1 in the new coordinate system was calculated and shown as heatmaps in Fig. 3. And we found that the spatial pattern of incident locations at the population level presented an obvious bi-central aggregation feature.

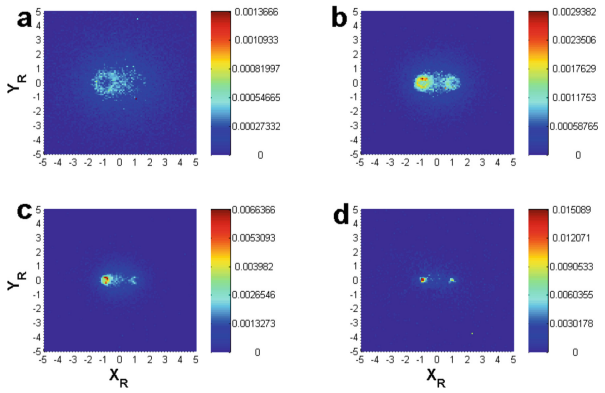

Fig. 3. Heatmap of the number of emergency calls in a relative coordinate system for four groups commuting distance.

To uncover the spatial patterns of the relative positions of emergency call behavior, we classified each incident location to its closer reference center (home or workplace). Then some statistics described in Subsect. 2.2 were calculated for further study. The distributions of D_h and D_w were shown in Fig. 4 (a) and (b), respectively. We tested the fitness of these two distributions with functions of power-law (POW), exponent (EXP), truncated power-law (TPL) and gauss (GAU). It was shown that $P(D_h)$ and $P(D_w)$ could be well fitted by the Gaussian function $P(x) = \frac{A}{\sqrt{2\pi}\sigma}\exp\left(-\frac{(x+\mu)^2)}{2\sigma^2}\right)$, where $A = 31.02, \mu = -18.98, \sigma = 10.04$ for $P(D_h)$ and $A = 15.42, \mu = -14.30, \sigma = 9.36$ for $P(D_w)$.

Figure 4 (c) showed the distributions of θ_h and θ_w, and the results were represented by blue circles and red triangles, respectively. The characteristics of $P(\theta_w)$ and $P(\theta_h)$ were consistent, which can be fitted by the Fourier

series $f(x) = a_0 + a_1\cos(\omega x) + b_1\sin(\omega x) + a_2\cos(\omega x) + b_2\sin(\omega x)$, where $a_0 = 0.014, a_1 = -0.0044, b_1 = 0.0037, a_2 = 0.0046, b_2 = 0.00085, \omega = 0.017$. The results indicate that the incident locations are mainly concentrated in the vicinity of the commuting direction.

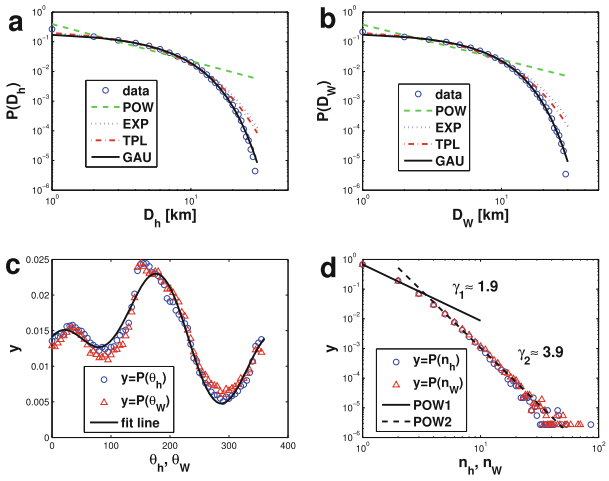

Fig. 4. (a) and (b) are the distribution of D_h and D_w, separately. A power-law distribution (the green dashed line), an exponential distribution (blue dot line), an exponentially truncated power-law distribution (red dashed line) and a Gaussian distribution (black line) of the two indicators are shown for fitting. (Color figure online)

In order to investigate whether the central reference point of the emergency call behavior is random, we analyzed the incident location series around home and workplace separately. Real data shows that the overall number of emergency calls around the two centers is almost equal. For an individual, the consecutive times of home (workplace) in the reference center sequence is identified by $n_h(n_w)$. If the conversion process of reference centers is random, the probability distribution $P(n_h)$ and $P(n_w)$ will appear exponential decay at the aggregated level. However, as shown in Fig. 4 (d), the patterns of $P(n_h)$ and $P(n_w)$ show two segments of the power-law decay, and the exponents are $\gamma_1 \approx 1.9$ and $\gamma_2 \approx 3.9$, where the inflection point is at 3. It indicates that the reference center of the incident locations where an individual makes emergency calls has a certain memory effect. That will provide a reference for our work on model construction.

4 Model

Based on the above results, the incident locations are mainly close to one's home or workplace. The distribution of the total number of these locations obeys a

power-law decay with memory effect. The displacement and the radius of gyration of trajectories obey a Gaussian distribution at aggregation level, respectively. Accordingly, a model of Double Center Memory effect Random Walk (DCMRW) was proposed to generate the spatial series of emergency call behavior. Figure 5 (a) shows the simulation mechanism of the model which is assumed as follows:

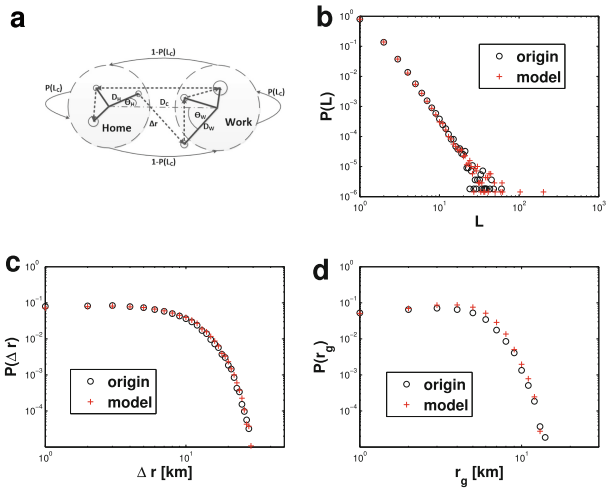

Fig. 5. (a) The DCMRW model. (b), (c) and (d) are the statistical characteristics of real data (origin) and simulation results (model) for comparison.

(1) Each individual has a unique home and workplace, and D_c is identified as the commuting distance, which obeys an exponential distribution $D_c \sim \text{Exp}(\lambda)$;
(2) The locations where individual makes an emergency call are switched by the memory process, and the total number of these locations (L) is generated by the following memory function:

$$p(L) = \left(\frac{L}{L+1}\right)^{\nu}, \tag{6}$$

where ν is the parameter to control the memory strength;
(3) $\pi_h(\pi_w)$ is the probability of home (workplace) as the center for data generation, and $0 \leq \pi_h \leq 1$ ($\pi_w = 1 - \pi_h$). The model with $\pi_h = 0$ or $\pi_h = 1$ would become a single-center random walk model;
(4) The generation of consecutive incident locations for emergency call behavior around a center is effected by a memory process, and the number of these locations L_c is generated by the following function:

$$p(L_c) = \left(\frac{L_c}{L_c+1}\right)^{\nu_c}, \tag{7}$$

where ν_c is the parameter to control the memory strength;

(5) The distance of an incident location away from home is generated by Gaussian distribution $D_h \sim N(\mu_h, \sigma_h)$ $(D_h \geq 0)$. And the distance from workplace obeys the Gaussian distribution $D_w \sim N(\mu_w, \sigma_w)$ $(D_w \geq 0)$ in the same way;

(6) The angle θ_h and θ_w obey the following Fourier function:

$$f(x) = a_0 + a_1\cos(\omega x) + b_1\sin(\omega x) + a_2\cos(\omega x) + b_2\sin(\omega x). \tag{8}$$

Through the simulation by model with parameters $\pi_H = 0.5, \lambda = 0.20, \nu = 2.28, \nu_c = 2.9, \mu_H = -19, \sigma_H = 10, \mu_w = -14.3, \sigma_w = 9.36, a_0 = 0.014, a_1 = -0.0044, b_1 = 0.0037, a_2 = 0.0046, b_2 = 0.00085, \omega = 0.017$, we collected about 1 million emergency call records from 0.5 million individuals. The spatial patterns of the real data can be well fitted by our simulation results as shown in Fig. 5 (b–d), which verified the effectiveness of the model.

Focusing on the parameters $\lambda, \nu, \nu_c, \mu_H, \sigma_H, \mu_w$ and σ_w, the fitting effect of simulation results generated by our model is measured by the method given in Subsect. 2.2. The referenced distributions include the probability distribution of the number of incident locations $P(L)$, the probability distribution of displacement $P(\Delta r)$ and the probability distribution of radius of gyration $P(r_g)$. As shown in Fig. 6–Fig. 9, the results (origin) of the real data, which is collected from $N = 100,000$ sampling individuals as a reference, are represented by black circles. The simulation results of model with different parameter values are represented by magenta triangle, yellow star, red cross, green square, blue diamond, etc. Detailed analyses of the parameters are as follows:

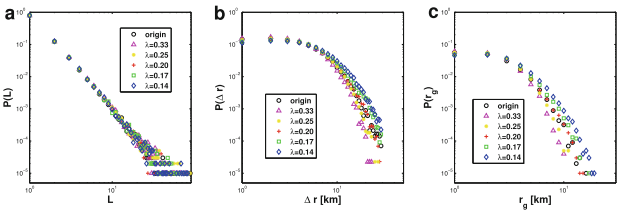

Fig. 6. The comparison of reproducing spatial patterns with different λ.

(1) λ: As shown in Fig. 6, λ has little effect on $P(L)$, but it has significant affect on the fitting goodness of the tail of $P(\Delta r)$ and $P(r_g)$. It indicates that with the increase of the average value of commute distance for agents, the generation probability of larger value of displacement and gyration radius will also increase. According to the results of KL-divergence given in Table 1, $\lambda = 0.20$ is the best choice for parameter to fit the real patterns, which means the average value of commute distance $\frac{1}{\lambda}$ in real data is about 5 km.

Table 1. The comparison of fitting results for reproducing spatial patterns by model with different λ.

λ	$D(P(L) \parallel Q(L\|\varphi))$	$D(P(\Delta_r) \parallel Q(\Delta_r\|\varphi))$	$D(P(r_g) \parallel Q(r_g\|\varphi))$	$\langle R \rangle$
0.33	5.9×10^{-4}	0.0430	0.0101	1.3900
0.25	3.9×10^{-4}	0.0232	0.0055	0.8076
0.20	$\mathbf{3.4 \times 10^{-4}}$	**0.0032**	**0.0003**	**0.3078**
0.17	3.6×10^{-4}	0.0342	0.0046	0.8466
0.14	4.9×10^{-4}	0.0662	0.0122	1.6479

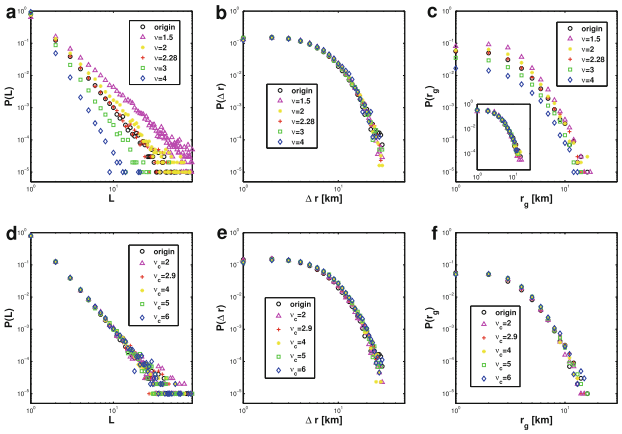

Fig. 7. The comparison of reproducing spatial patterns with different ν and ν_c.

Table 2. The comparison of fitting results for reproducing spatial patterns by the model with different ν.

ν	$D(P(L) \parallel Q(L\|\varphi))$	$D(P(\Delta_r) \parallel Q(\Delta_r\|\varphi))$	$D(P(r_g) \parallel Q(r_g\|\varphi))$	$\langle R \rangle$
1.5	0.1220	0.0105	0.0922	1.4408
2	0.0129	0.0142	0.0136	0.4965
2.28	**0.0003**	**0.0032**	**0.0003**	**0.0812**
3	0.0408	0.0078	0.0291	0.5746
4	0.1808	0.0328	0.1145	2.4069

Table 3. The comparison of fitting results for reproducing spatial patterns by the model with different ν_c.

ν_c	$D(P(L) \parallel Q(L\|\varphi))$	$D(P(\Delta_r) \parallel Q(\Delta_r\|\varphi))$	$D(P(r_g) \parallel Q(r_g\|\varphi))$	$\langle R \rangle$
2	4.0×10^{-4}	0.0052	0.0012	0.5895
2.9	$\mathbf{3.4 \times 10^{-4}}$	**0.0032**	**0.0003**	**0.3649**
4	4.4×10^{-4}	0.0232	0.0030	1.2415
5	4.8×10^{-4}	0.0286	0.0028	1.3419
6	5.4×10^{-4}	0.0284	0.0033	1.4622

(2) ν, ν_c: As shown in Fig. 7(a)-(c), ν has little effect on $P(\Delta r)$, but can affect the exponent of power-law function $P(L)$ and the proportion of the number of agents with small radius of gyration. It indicates that with the increase of ν, the memory effect on generation of incident locations will be stronger and the scope of emergency call activity for agents will also increase. As shown in Fig. 7(d)-(f), although ν_c potentially affects the memory strength of generation of incident locations around a single-center for an agent, it has no significant impact on patterns of $P(L)$, $P(\Delta r)$ and $P(r_g)$ at the aggregated level. According to the results of KL-divergence given in Table 2 and Table 3, the parameters $\nu \approx 2.28$ and $\nu_c \approx 2.9$ are the best choices for the model to fit the real patterns.

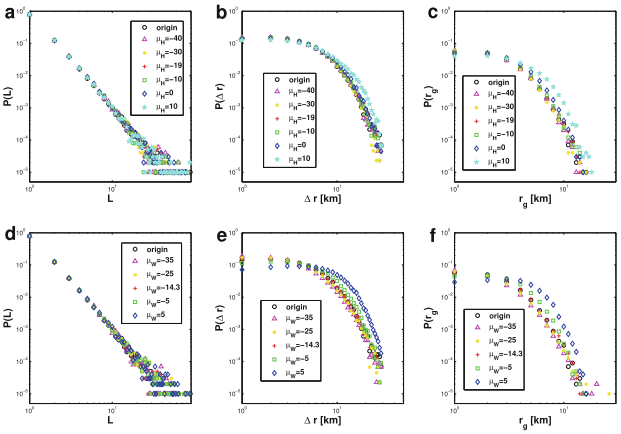

Fig. 8. The comparison of reproducing spatial patterns with different μ_H and μ_W.

Table 4. The comparison of fitting results for reproducing spatial patterns by the model with different μ_H.

μ_H	$D(P(L) \parallel Q(L\|\varphi))$	$D(P(\Delta_r) \parallel Q(\Delta_r\|\varphi))$	$D(P(r_g) \parallel Q(r_g\|\varphi))$	$\langle R \rangle$
−40	5.1×10^{-4}	0.0044	0.0005	0.4605
−30	5.4×10^{-4}	0.0035	0.0004	0.4548
−19	$\mathbf{3.4 \times 10^{-4}}$	**0.0032**	**0.0003**	**0.3117**
−10	5.7×10^{-4}	0.0051	0.0012	0.5476
0	4.7×10^{-4}	0.0122	0.0071	0.9113
10	6.1×10^{-4}	0.0574	0.0352	3.3143

(3) μ_H, μ_W: As shown in Fig. 8, μ_H and μ_W have no effect on $P(L)$. If $\mu_H > 0$ and $\mu_W > 0$, the distribution $P(\Delta r)$ and $P(r_g)$ for simulation data will deviate from real patterns significantly. Meanwhile, if $\mu_H < 0$ and $\mu_W < 0$, the spatial patterns of real data can be fitted well, but small μ_H and μ_W

Table 5. The comparison of fitting results for reproducing spatial patterns by the model with different μ_W.

μ_W	$D(P(L) \parallel Q(L\|\varphi))$	$D(P(\Delta_r) \parallel Q(\Delta_r\|\varphi))$	$D(P(r_g) \parallel Q(r_g\|\varphi))$	$\langle R \rangle$
-35	4.9×10^{-4}	0.0402	0.0061	0.6386
-25	5.2×10^{-4}	0.0167	0.0024	0.4912
-14.3	$\mathbf{3.4 \times 10^{-4}}$	**0.0032**	**0.0003**	**0.2646**
-5	4.7×10^{-4}	0.0404	0.0111	0.7159
5	4.9×10^{-4}	0.2842	0.0718	2.8898

will cause the simulation to generate a large number of negative samples which will be discarded. According to the results of KL-divergence given in Table 4 and Table 5, the parameter $\mu_H \approx -19$ and $\mu_W \approx -14.3$ are the best choices for model to fit the real patterns.

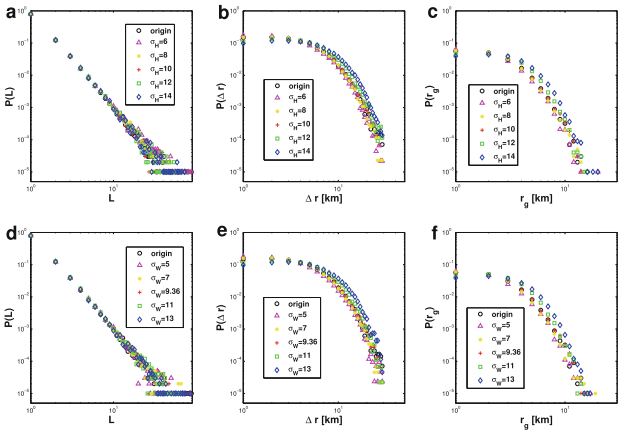

Fig. 9. The comparison of reproducing spatial patterns with different σ_H and σ_W.

(4) σ_H, σ_W: As shown in Fig. 9, σ_H and σ_W have no effect on $P(L)$. If the values of σ_H and σ_W are large, the distribution $P(\Delta r)$ and $P(r_g)$ for simulation data will deviate from real patterns significantly. Meanwhile, if σ_H and σ_W are small, spatial patterns of real data can be fitted well, but it will also cause the simulation to generate a large number of negative samples which will be discarded. According to the results of KL-divergence given in Table 6 and Table 7, the parameters $\sigma_H \approx 10$ and $\sigma_W \approx 9.36$ are the best choices for the model to fit the real patterns.

Table 6. The comparison of fitting results for reproducing spatial patterns by the model with different σ_H.

σ_H	$D(P(L) \parallel Q(L\|\varphi))$	$D(P(\Delta_r) \parallel Q(\Delta_r\|\varphi))$	$D(P(r_g) \parallel Q(r_g\|\varphi))$	$\langle R \rangle$
6	4.9×10^{-4}	0.0151	0.0021	0.6237
8	3.6×10^{-4}	0.0041	0.0004	0.3416
10	$\mathbf{3.4 \times 10^{-4}}$	**0.0032**	**0.0003**	**0.3129**
12	4.5×10^{-4}	0.0477	0.0092	1.2171
14	4.6×10^{-4}	0.1121	0.0242	2.5047

Table 7. The comparison of fitting results for reproducing spatial patterns by the model with different σ_W.

σ_W	$D(P(L) \parallel Q(L\|\varphi))$	$D(P(\Delta_r) \parallel Q(\Delta_r\|\varphi))$	$D(P(r_g) \parallel Q(r_g\|\varphi))$	$\langle R \rangle$
5	5.0×10^{-4}	0.0217	0.0037	0.6889
7	5.6×10^{-4}	0.0039	0.0013	0.4571
9.36	$\mathbf{3.4 \times 10^{-4}}$	**0.0032**	**0.0003**	**0.2633**
11	7.4×10^{-4}	0.0451	0.0085	1.2740
13	4.3×10^{-4}	0.1080	0.0234	2.3168

5 Conclusions

It is of great importance to capture and simulate human behavior to understand the internal mechanism of an emergency. Nowadays, electronic footprint data provides necessary materials for revealing the impact of emergencies on human behavior patterns. This paper explored the spatial patterns of emergency calls made by citizens in a metropolitan city in China using emergency call records and mobile phone signaling data. By measuring the spatial statistical characteristics of emergency calls, we find that there is a strong randomness in this behavior, but the number of emergency calls made by an individual in a specific location follows a power-law distribution, and the spatial pattern of incident locations presents a bi-central aggregation feature. These patterns provide the possibility to predict the trajectory of emergency call behavior. Then we propose an agent based model named DCMRW for the generation of incident location series. The effectiveness of the generation mechanism of our model has been verified by simulation experiments.

Our work could benefit to improve the efficiency of emergency management from the following aspects: situation analysis, resource allocation and police deployment.

References

1. Altshuler, Y., et al.: The social amplifier—reaction of human communities to emergencies. J. Stat. Phys. **152**(3), 399–418 (2013). https://doi.org/10.1007/s10955-013-0759-z

2. Bagrow, J.P., Wang, D., Barabási, A.L.: Collective response of human populations to large-scale emergencies. PLoS ONE **6**(3), e17680 (2011). https://doi.org/10.1371/journal.pone.0017680
3. Barabási, A.L.: The origin of bursts and heavy tails in human dynamics. Nature **435**(7039), 207–211 (2005). https://doi.org/10.1038/nature03459
4. Barrientos, F., Sainz, G.: Interpretable knowledge extraction from emergency call data based on fuzzy unsupervised decision tree. Knowl. Based Syst. **25**(1), 77–87 (2012). https://doi.org/10.1016/j.knosys.2011.01.014
5. Becker, R., et al.: Human mobility characterization from cellular network data. Commun. ACM **56**(1), 74 (2013). https://doi.org/10.1145/2398356.2398375
6. Brockmann, D., Hufnagel, L., Geisel, T.: The scaling laws of human travel. Nature **439**(7075), 462–465 (2006). https://doi.org/10.1038/nature04292
7. Candia, J., González, M.C., Wang, P., Schoenharl, T., Madey, G., Barabási, A.L.: Uncovering individual and collective human dynamics from mobile phone records. J. Phys. A: Math. Theor. **41**(22), 224015 (2008). https://doi.org/10.1088/1751-8113/41/22/224015
8. Chu, J., et al.: Passenger demand prediction with cellular footprints. IEEE Trans. Mob. Comput. **21**(1), 252–263 (2022). https://doi.org/10.1109/TMC.2020.3005240
9. Eriksson, M.: Conceptions of emergency calls: emergency communication in an age of mobile communication and prevalence of anxiety. J. Contingencies Crisis Manag. **18**(3), 165–174 (2010). https://doi.org/10.1111/j.1468-5973.2010.00613.x
10. Freudendal-Pedersen, M., Kesselring, S.: What is the urban without physical mobilities? COVID-19-induced immobility in the mobile risk society. Mobilities **16**(1), 81–95 (2021). https://doi.org/10.1080/17450101.2020.1846436
11. Gao, L., Song, C., Gao, Z., Barabási, A.L., Bagrow, J.P., Wang, D.: Quantifying information flow during emergencies. Sci. Rep. **4**, 3997 (2014). https://doi.org/10.1038/srep03997
12. Jasso, H., Fountain, T., Baru, C., Hodgkiss, W., Reich, D., Warner, K.: Spatiotemporal analysis of 9-1-1 call stream data. In: Proceedings of the 2006 International Conference on Digital Government Research, pp. 21–22. Digital Government Society of North America (2006). https://doi.org/10.1145/1146598.1146608
13. Jasso, H., Fountain, T., Baru, C., Hodgkiss, W., Reich, D., Warner, K.: Prediction of 9-1-1 call volumes for emergency event detection. In: Proceedings of the 8th Annual International Conference on Digital Government Research: Bridging Disciplines & Domains, pp. 148–154. Digital Government Society of North America (2007)
14. Jasso, H., Hodgkiss, W., Baru, C., Fountain, T., Reich, D., Warner, K.: Spatiotemporal characteristics of 9-1-1 emergency call hotspots. In: Proceedings of the National Science Foundation Symposium on Next Generation of Data Mining and Cyber-Enabled Discovery for Innovation (NGDM 2007), pp. 10–12. Citeseer (2007)
15. Jasso, H., Hodgkiss, W., Baru, C., Fountain, T., Reich, D., Warner, K.: Using 9-1-1 call data and the space-time permutation scan statistic for emergency event detection. Gov. Inf. Q. **26**(2), 265–274 (2009). https://doi.org/10.1016/j.giq.2008.12.005
16. Kenett, D.Y., Portugali, J.: Population movement under extreme events. Proc. Natl. Acad. Sci. **109**(29), 11472–11473 (2012). https://doi.org/10.1073/pnas.1209306109
17. Kung, K.S., Greco, K., Sobolevsky, S., Ratti, C.: Exploring universal patterns in human home-work commuting from mobile phone data. PLoS ONE **9**(6), e96180 (2014). https://doi.org/10.1371/journal.pone.0096180

18. Lin, Y.-R., Margolin, D.: The ripple of fear, sympathy and solidarity during the Boston bombings. EPJ Data Sci. **3**(1), 1–28 (2014). https://doi.org/10.1140/epjds/s13688-014-0031-z
19. Lu, X., Bengtsson, L., Holme, P.: Predictability of population displacement after the 2010 Haiti earthquake. Proc. Natl. Acad. Sci. **109**(29), 11576–11581 (2012). https://doi.org/10.1073/pnas.1203882109
20. Moumni, B., Frias-Martinez, V., Frias-Martinez, E.: Characterizing social response to urban earthquakes using cell-phone network data: the 2012 Oaxaca earthquake. In: Proceedings of the 2013 ACM Conference on Pervasive and Ubiquitous Computing Adjunct Publication, pp. 1199–1208. UbiComp 2013 Adjunct, ACM, New York (2013). https://doi.org/10.1145/2494091.2497350
21. Pastor-Escuredo, D., et al.: Flooding through the lens of mobile phone activity. In: Global Humanitarian Technology Conference (GHTC 2014), pp. 279–286. IEEE (2014). https://doi.org/10.1109/GHTC.2014.6970293
22. Preis, T., Moat, H.S., Bishop, S.R., Treleaven, P., Stanley, H.E.: Quantifying the digital traces of hurricane Sandy on Flickr. Sci. Rep. **3**(1), 1–3 (2013). https://doi.org/10.1038/srep03141
23. Song, X., Zhang, Q., Sekimoto, Y., Horanont, T., Ueyama, S., Shibasaki, R.: Modeling and probabilistic reasoning of population evacuation during large-scale disaster. In: Proceedings of the 19th ACM SIGKDD International Conference on Knowledge Discovery and Data Mining (KDD 2013), pp. 1231–1239. ACM, New York (2013). https://doi.org/10.1145/2487575.2488189
24. Song, X., Zhang, Q., Sekimoto, Y., Shibasaki, R.: Prediction of human emergency behavior and their mobility following large-scale disaster. In: Proceedings of the 20th ACM SIGKDD International Conference on Knowledge Discovery and Data Mining (KDD 2014), pp. 5–14. ACM, New York (2014). https://doi.org/10.1145/2623330.2623628
25. Szell, M., Grauwin, S., Ratti, C.: Contraction of online response to major events. PLoS ONE **9**(2), e89052 (2014). https://doi.org/10.1371/journal.pone.0089052
26. Traag, V.A., Browet, A., Calabrese, F., Morlot, F.: Social event detection in massive mobile phone data using probabilistic location inference. In: 2011 IEEE Third International Conference on Privacy, Security, Risk and Trust (PASSAT) and 2011 IEEE Third Inernational Conference on Social Computing (SocialCom), pp. 625–628 (2011). https://doi.org/10.1109/PASSAT/SocialCom.2011.133
27. Wang, Q., Taylor, J.E.: Quantifying human mobility perturbation and resilience in hurricane Sandy. PLoS ONE **9**(11), e112608 (2014). https://doi.org/10.1371/journal.pone.0112608
28. Wang, W., et al.: Temporal patterns of emergency calls of a metropolitan city in China. Phys. A Stat. Mech. Appl. **436**, 846–855 (2015). https://doi.org/10.1016/j.physa.2015.05.028
29. Woolley-Meza, O., Grady, D., Thiemann, C., Bagrow, J.P., Brockmann, D.: Eyjafjallajökull and 9/11: the impact of large-scale disasters on worldwide mobility. PLoS ONE **8**(8), e69829 (2013). https://doi.org/10.1371/journal.pone.0069829
30. Xu, F., Li, Y., Jin, D., Lu, J., Song, C.: Emergence of urban growth patterns from human mobility behavior. Nat. Comput. Sci. **1**(12), 791–800 (2021). https://doi.org/10.1038/s43588-021-00160-6